Predicting between-subject variability of brain activities based on brain structure

Xiao XIANG†, Yusuke YAMAMOTO††, Makoto P. KATO†, and Katsumi TANAKA†

† Graduate School of Informatics, Kyoto University
†† Graduate School of Management, Kyoto University
Yoshida Honmachi, Sakyo-ku, Kyoto, 606-8501, Japan
E-mail: †{kou,kato,tanaka}@dl.kuis.kyoto-u.ac.jp, ††yamamoto@gsm.kyoto-u.ac.jp

Abstract We present an approach to estimate task-evoked fMRI data based on structural MRI in order to reveal in which level individual differences of brain activities can be explained by brain structure. We extract regions of interest and conducted voxel-based morphometry analysis on both fMRI and structural MRI data, and apply a supervised machine learning approach to capture the correspondence between them. Experiments were conducted with fMRI data for gambling and emotion processing tasks, which tend to show remarkable difference between individuals.

Key words neuroimage, data mining, brain

1. Introduction

With the development of neuroimaging techniques [1], especially magnetic resonance imaging(MRI) and functional magnetic resonance imaging(fMRI), researchers have been able to observe both brain structure and brain neurobiological activity in higher temporal and spatial resolution. MRI scanners play strong magnetic fields on brain in order to detect different intensity of resonant electromagnetic waves radiated by hydrogen atom so that tissues can be distinguished by their various water content and whole brain image is generated [2]. The fMRI concept builds on the earlier MRI scanning technology and the discovery of properties of oxygen-rich blood, which is property shows brain activities are closely linked to blood flow and blood oxygenation in the brain. Similarly, fMRI scanners detect different intensity of resonant electromagnetic waves radiated by hemoglobins in various reduction level to find active regions of brain, which are consuming more oxygencan [3].

Ordinary analysis in fMRI usually lay emphasis on common correspondences between brain functions/behaviors and neurobiological brain activities of subjects. For instance, Fossati *et al.* carried out an experiment [4], in which ten healthy subjects were presented with words describing positive and negative personality traits during fMRI scanning. The results provide evidence that self-reference is mainly contributed by right dorsomedial prefrontal cortex. However, most of the existing fMRI experiments explored brain activities common for all participates, while their between-subject variability has not been analyzed in depth. However, the between-subject variability may imply the individual differences of mental processes for the same stimulus. In a study using fMRI, Mariko Osaka *et al.* selected two labeled groups, one has high score in working memory capacity while another is lower, as experiment subjects to record their brain activities [5]. The results indicate that the attention controlling system is more effective in higher scored group compared to that of lower group. Prediction the between-subject variability for a certain stimulus is useful to realize highly personalized services such as advertisements and medical consultation.

In this paper, we tackle the problem of predicting individual brain activities based on brain structure data. To specify the scope of the problem, we employ task-evoked fMRI data as record of brain activities during certain tasks and structural MRI data as brain structure data of subjects. In view of greater granularity and more explainable, we extract dozens of region of interest(ROI) from both MRI data and fMRI data. By applying Voxel-based morphometry analysis, we compress MRI data into first-order vector. Finally, based on MRI vector, we predict possible values of each ROI of the same subject to one stimulus, using support-vector machine(SVM).

We present our experiment on WU-Minn HCP [6] dataset, which includes 500 subjects' MRI and task-evoked fMRI data. We focus on gamble and emotion processing task and give prediction of every stimulus to each subject and estimate mean accuracy.

In this paper, Section 2 introduces several representative studies on task-evoked fMRI and studies combining neuroimaging and informatics techniques. Section 3 describes the general model in which we predict fMRI data based on MRI data. We explains procedure and result of our experiment in Section 4. Finally, conclusions was drawn in last section.

2. Related Work

Classic studies in the field of task-evoked fMRI are usually in a form of testing hypotheses through observing brain responses to a certain stimulus. In an reward-related fMRI experiment [7] conducted by Itzhak *et al.*, researchers showed discrete categories of beautiful faces as stimuli to human subjects and scanned active brain regions using fMRI scanner. The results suggest that passive viewing of beautiful female faces activates reward circuitry(a bunch of brain regions related to certain brain function) and the circuitry does not include aesthetic assessment in all subjects. In a study conducted by Naomi *et al.* [8], researchers tried to find if brain bases of social pains are similar to those of physical pain by checking if the same regions in subjects' brains are activated to social and physical pain stimuli. In addition, Joshua *et al.* [9] applied two fMRI experiments using moral dilemmas as probes and argued that in moral judgment, emotional processing also plays an important role. Another stream of research lays emphasis on the connectivity between brain regions. For instance, Qin *et al.* [10]demonstrated a brain network implicated in both pain sensation and pain modulation, by performing statistical covariance analysis. Jonas *et al.* [11] presented an approach based on polythetic decision trees to find and classify frequency subbands in the brain. Smith gives a review on area of fMRI connectivity. [12] After voxel-based morphometry(VBM) [13] analysis was proposed, a number of studies on the correlation between brain structure and human personality or human behavior patterns have been published in the literature. Good *et al.* [14] utilized VBM to examine the effects of age on brain matters in 465 normal adults. Baron *et al.* [15] conducted an analysis on the gray matter density by means of VBM on both patients with Alzheimer's disease and healthy subjects, finding that significant clusters of gray matter were lost in the patient group. Cadenhead *et al.* [16] showed the magnitude of placebo analgesia is related to the gray matter density in several brain regions. Studies centered on remarkable between-subject differences, such as anatomical variability between patients and healthy subjects. Recently, some researchers have tackled prediction of subjects' personality or behavior patterns based on the brain structure. Kanai *et al.* [17] predicted the number of friends on a social networking service by utilizing the grey matter density in specific brain regions. In a VBM study on personality, Hu *et al.* [18] investigated the correlation between the five-factor model (FFM) personality traits and brain structure. Zhou *et al.* [19] showed neurobiological evidences on brain matter abnormalities in an internet addiction group. A study focusing on gender difference in online trust shows that male and female subjects activate gender-independent brain regions when exposed to eBay offers, which indicates that the brain regions that encode trustworthiness differ between women and men [20]. These papers tried to demonstrate that between-subject differences can be used as a source of information to link human behaviours and cognition to the brain anatomy. Kanai and Rees [21] provided a meta-analysis on this topic. However, most of the studies in this field have ignored the intermediate section in the ternary relation of the brain structure, brain activities, personality. In other words, the correlation between brain structure and brain activities have not extensively analyzed in the existing work.

An attempt to explore the relationship between brain structure and activities has been initiated by Yi *et al.* [22], who observed both structural and functional variability using VBM analysis and analysis on default mode network fMRI data. Whereas, the relationship between the brain structure and task-evoked fMRI data has not been explored and is the main interest of this paper.

3. Methodology

3.1 Problem Definition

Structural MRI and functional MRI data is usually composed of million of voxels, each of which indicates the intensity of the electromagnetic wave at a certain location of the brain (and at a certain time point in the case of functional MRI data). Therefore, structural MRI data for a particular subject are represented by a third-order tensor $\mathbf{X} \in \mathbb{R}^{W \times H \times D}$ where W, H, and D are the width, height, and depth of a MRI scan. In a similar way, functional MRI data for a particular subject are represented by a forth-order tensor $\mathbf{Y} \in \mathbb{R}^{W \times H \times D \times T}$ where T is the total number of time points. The problem of predicting function MRI data based on structural MRI data $\mathbf{X}$ can be formalized as follows:

$$\hat{\mathbf{Y}} = f(\mathbf{X}) \tag{1}$$

where $\hat{Y}$ ($\in \mathbb{R}^{W \times H \times D \times T}$) is *predicted* functional MRI data, and f is a function such that $f : \mathbb{R}^{W \times H \times D} \rightarrow \mathbb{R}^{W \times H \times D \times T}$. If we can find a function that achieves reasonably small loss between the predicted and *observed* functional MRI data, we can argue that there is strong correlation between brain structure and activities.

Although our conceptual problem definition was presented

above, it is infeasible to solve such a regression problem with high dimensional input and output. Thus, we introduce a simplified version of the regression problem below. Suppose that functions Φ_s and Φ_f can extract some features from structural MRI data $\mathbf{X}$ and functional MRI data $\mathbf{Y}$, and output K_s- and K_f-dimensional vectors, respectively. Then, the problem described in Equation (1) can be simplified as follows:

$$\hat{\mathbf{y}} = f(\Phi_s(\mathbf{X})) \tag{2}$$

where f is a function defined as $f : \mathbb{R}^{K_s} \rightarrow \mathbb{R}^{K_f}$, and $\hat{\mathbf{y}}$ is prediction for $\Phi_f(\mathbf{Y})$, a vector for function MRI data $\mathbf{Y}$. Thus, our purpose is to find a function f that minimizes the difference between $\hat{\mathbf{y}}$ and $\Phi_f(\mathbf{Y})$, which can be measured by a loss function $l : \mathbb{R}^{K_f} \times \mathbb{R}^{K_f} \rightarrow \mathbb{R}$. Here, Φ_f and Φ_s can be ROI extraction. Each ROI represents a structural related tissues having similar function, which can be helpful to interpret the experiment results later. For example, when we find subjects have much grey matters in ROI A and their ROI B are likely to be activated by a certain stimulus, we can provide more convincing explanation based on anatomically or functionally relationship, which have been revealed by previous neurobiology works, between ROI A and ROI B.

3. 2 Extracting ROI

We have two types of data, structural data from MRI scanning and functional data from fMRI scanning. Extracting ROIs and performing volume calculating in case of structural data will be discussed in Section 3.2.1. Extracting ROI from functional data, which involves two extracting methods, will be discussed in Section 3.2.2.

We apply previously prepared masks on MRI image of each subjects basing on prior probability maps, in order to distinguish each brain structure, such as hippocampus, subcortical nuclei or inferior frontal gyrus. This preprocessing can be expressed as:

$$\mathbf{X}_i = \mathbf{X} \cdot \mathbf{M}_i \tag{3}$$

where $\mathbf{X}$ is structural data. $\mathbf{M}_i$ is the ith ROI mask which is a third-order binary tensor, the value of voxels in the region we want to extract is 1 while the left is 0. $\cdot$ is a tensor product defined as following:

$$\mathbf{A} \cdot \mathbf{B} = (a_{ijk} \cdot b_{ijk})_{1 \leqq i \leqq m, 1 \leqq j \leqq n, 1 \leqq k \leqq o} \tag{4}$$

where $\mathbf{A}, \mathbf{B} \in \mathbb{R}^{\{m \times n \times o\}}$. After ROI extraction, volume of all ROIs in subjects' brain can be obtained by doing VBM analysis on preprocessed MRI image. VBM analysis excelled traditional method by registering brain to a template, which gets rid of remarkable difference in brain anatomy among subjects. Hence, each voxel represents the average of itself and its neighbors, therefore, comparison can be done across same ROI from different subjects at every voxel. VBM analysis can be summarized succinctly as the following 4 steps:

- Segment MRI image, to identify grey matter (GM), white matter (WM) and cerebrospinal fluid (CSF) using Gaussian mixture model prior distribution. For different types of brain matter, three segmented images for each raw image are generated.
- Estimate the segmentation by align the segmented images together and iteratively registering the raw image with their average
- Generate spatially normalized and smoothed Jacobian scaled segmented images, using the segmentation estimated in the previous step
- Compute GM, WM, CSF volume of each ROI by calculating the voxels in segmented images.

Finally, we affine all these volumes into first-order vector as a structural feature vector to one subject. Let x_i be the calculated volume from $\mathbf{X}_i$ data then the VBM and affining procedures can be expressed as follows:

$$x_i = \sum_{\mathbf{V} \in \mathbf{X}_i} vol_{\mathbf{V}} \tag{5}$$

where $vol_{\mathbf{V}}$ is the volume of a voxel in the ith ROI. Naturally, the whole procedure Φ_s can be expressed in one formulation:

$$x_i = \sum_{\mathbf{V} \in \mathbf{X} \cdot \mathbf{M}_i} vol_{\mathbf{V}} \tag{6}$$

and with k disjoint ROIs, we obtain k-dimenstions vector $\mathbf{X}_j$ for jth subject:

$$\mathbf{X}_j = (x_1, x_2, ...x_k) \tag{7}$$

3. 2. 1 Extracting ROI from functional data

In case of functional data, we extract ROIs firstly by clustering the relatively more active regions in order to drop other regions with low information value. This clustering procedure can be simply represented as follows:

$$\mathbf{Y}_j = \mathbf{Y} \cdot \mathbf{M}_{\mathbf{f}j} \tag{8}$$

where $\mathbf{Y}$ is functional data and $\mathbf{M}_{\mathbf{f}j}$ is the jth functional ROI mask computed by clustering. The disadvantages are that we have had to use a whole run of data to define the ROI and that functional ROIs can be noisy, when the activation signal is not strong. An alternative is to use the anatomy of the brain to estimate the location of functional areas, which has been introduced in section 3.2.1. Let $\mathbf{Y}'$ be the both functional and structural extracted ROI tensor:

$$\mathbf{Y}' = \mathbf{Y} \cdot \mathbf{M}_{\mathbf{f}} \cdot \mathbf{M}_{\mathbf{s}} \tag{9}$$

where $\mathbf{M}_{\mathbf{f}}$ is functional ROI mask and $\mathbf{M}_{\mathbf{s}}$ is structural ROI

mask. Further, data is remain fourth-order tensor due to time-series information after extraction. Thus, we perform dimension reduction on the data by taking the mean of the electromagnetic intensity of voxels in ROI $\mathbf{Y}'$. Let y'_t be the average intensity of a ROI to a certain stimulus:

$$y = avg(\sum_{\mathbf{V}\in\mathbf{Y}'} int_{\mathbf{V}}) \tag{10}$$

where $int_{\mathbf{V}}$ is the intensity of the a voxel in ROI $\mathbf{Y}'$ and avg takes the average of intensities of all voxel in this ROI. Finally, we obtain one value for one ROI we extracted to a certain stimulus, and with k disjoint ROIs, we obtain k-dimensions vector $\mathbf{Y}_j$ for jth subject:

$$\mathbf{Y}_j = (y_1, y_2, ...y_k) \tag{11}$$

We combine X_j and Y_j as a data point of collection D, which can be expressed as $D = \{(\mathbf{X}_1, \mathbf{Y}_1)...(\mathbf{X}_j, \mathbf{Y}_j)...(\mathbf{X}_n, \mathbf{Y}_n)\}$ for n is the size of samples.

3.3 Prediction

Selection for classifier depends on what we actually want to predict. In section 3.2.2, we reduct raw data to scalars without category, therefore, it becomes a regression problem. Support Vector Machine (SVM), as an adaptable supervised learning model in machine learning, is widely used in regression. In a study on testing performance of 179 classifiers [23], results also show that SVM and random forest (RF) are most likely to be the best. We choose SVM as our estimator to make prediction and examine the accuracy. We map the collection D into k subsets for k ROIs and for ith ROI, we have $D_i = \{(\mathbf{X}_1, y_{1,i}), (\mathbf{X}_2, y_{2,i})...(\mathbf{X}_n, y_{n,i})\}$, where $y_{j,i}$ is y of ith ROI of jth subject. For each ROI we train a estimator f_i:$\mathbb{R}^k \rightarrow \mathbb{R}$. Finally we can combine all the estimators into one as a global estimator for all k ROIs, in other word, whole brain.

4. Experiment

4.1 Experiment Introdcution

In WU-Minn HCP dataset, there are massive data including personality, family background, behavior data, MR scanning data of 500 subjects. We mainly deal with the MRI data and task-evoked fMRI data. Table 1 provides basic parameters for the structural MRI session and Table 2 provides a list of the fMRI scans we use in our experiment.

The gambling task is adapted from one developed by Delgado *et al.* [24]. Subjects play a number guessing game while being scanned. In this game, subjects will win or lose money according to their answer by button-click for indicating if they think the number on the mystery card is bigger or smaller than 5 (ranging from 1-9). After each guess, they will get positive/negative/neutral feedbacks on screen. The

Table 1: Structural session

Type	TR(ms)	TE(ms)	TI(ms)	Voxel Size	Acquisition Description Time (min:sec)
T1w	2400	2.14	1000	0.7 mm isotropic	7:40
T2w	3200	565		0.7 mm isotropic	8:24

Table 2: Task-evoked fMRI

Task	Runs	Frames per run	Run Duration
Gambling	2	253	3:12
Language	2	316	3:57
Social Cognition	2	274	3:27
Emotion Processing	2	176	2:16

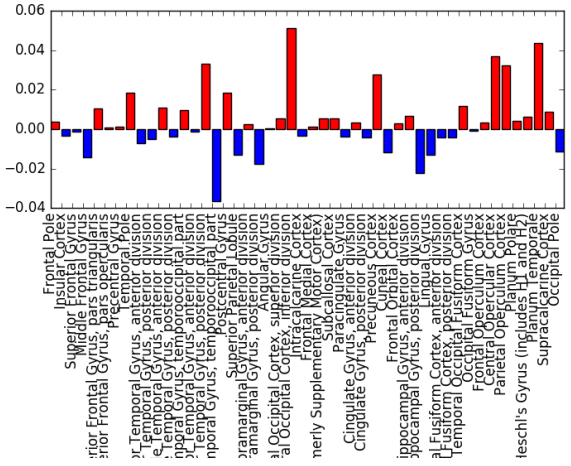

Figure 1: Pred_score of all 48 areas in **Language task**: areas with red bars are relatively predicable

experiment is block-designed in order to distinguish each response of subjects' brain to stimulus. In another experiment adapted from one developed by hariri *et al.*[25], subjects are presented with blocks of trials that either ask them to decide which of two faces presented on the bottom of the screen match the face at the top of the screen, or which of two shapes presented at the bottom of the screen match the shape at the top of the screen. The faces have an angry or fearful expression. There are 7 fMRI scans for 7 different types of tasks in HCP dataset. We pick up 4 tasks and their fMRI data from all 7 tasks for the reason that we consider that in these two tasks probably reflect more inter-individual variety and show differences in thinking patterns not knowledge or experience.

MRI and 4 types of fMRI dataset of 100 unrelated subjects were used. We selected Harvard-Oxford Atlas (Figure 1) as the mask to extract 48 ROIs.

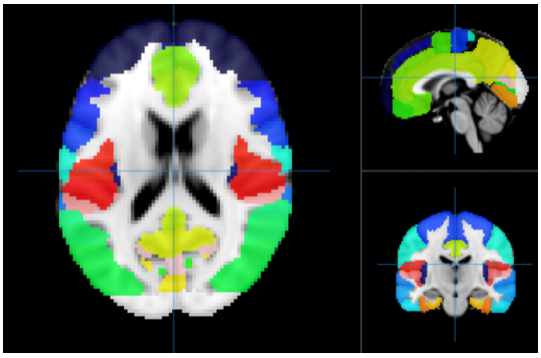

Figure 2: Harvard-Oxford Atlas: divide whole brain into 48 disjoint ROIs

To evaluate the predictability of each ROIs, we give a definition of predicable score as following:

$$Pred\_score_i = \frac{\sum_{j=1}^{n-p}(y_{j,i} - \frac{1}{p}\sum_{k=1}^{p} y_{k,i})^2}{\sum_{j=1}^{n-p}(y_{j,i} - f_i(\mathbf{X}_j))^2} - 1 \qquad (12)$$

where n is the number of subjects, p is the size of training set, $n-p$ is the size of test size. The numerator of this formulation shows the differences between average predictions and observed values while the denominator is the differences between our values predicted by our model and the observed values. Hence, one ROI is more predictable when its *pred_score* is larger. Especially, the ROI whose *pred_score* is lower than zero, is hardly able to be predicted.

4.2 Predicable Areas

Figure 1, 3, 4, 5 show *pred_score* of all 48 regions of all 4 tasks.

We find not all ROIs are easy to predict, which is explicable since only a few ROIs take part in one certain task. In Table 3, we list 3 ROIs, whose *pred_score* is highest, for each of the 4 tasks.

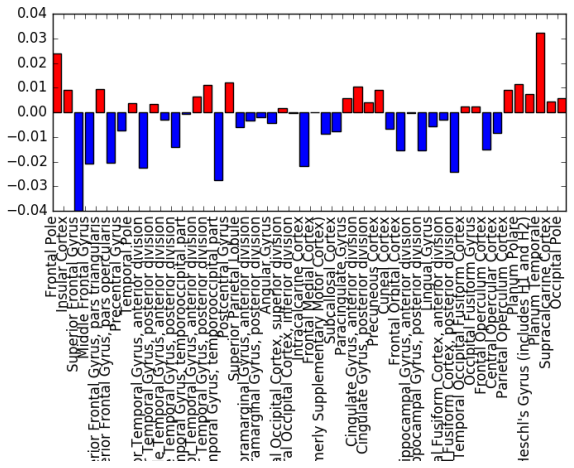

Figure 3: Pred_score of all 48 areas in **Emotion task**: areas with red bars are relatively predicable

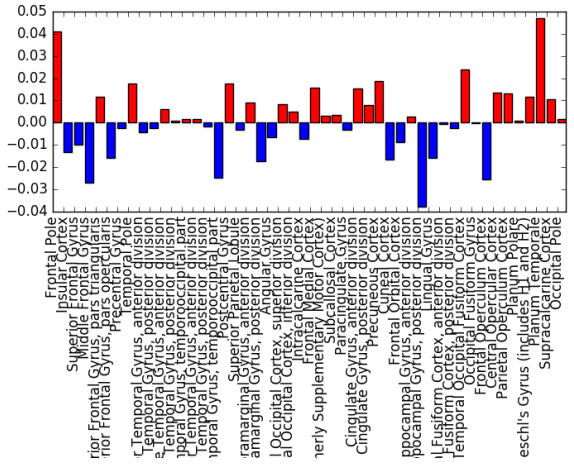

Figure 4: Pred_score of all 48 areas in **Social cognition task**: areas with red bars are relatively predicable

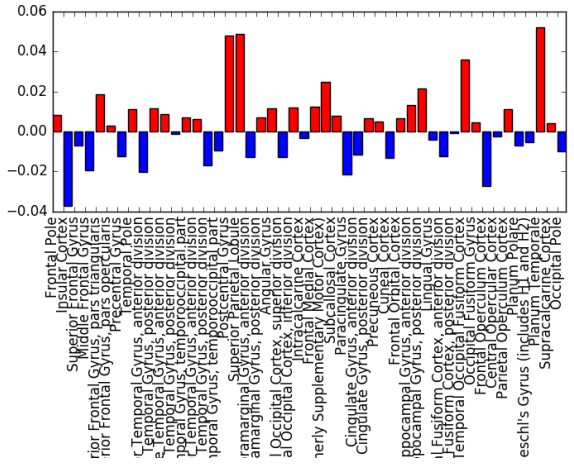

Figure 5: Pred_score of all 48 areas in **Gambling task**: areas with red bars are relatively predicable

Table 3: Top3 predicable ROIs: areas with **BOLD** font are unique areas that are not so predicable in other tasks

Task	Top1	Top2	Top3
Gambling	Planum Temporale	Postcentral Gyrus	**Superior Parietal Lobule**
Language	**Lateral Occipital Cortex, inferior division**	Planum Temporale	Central Opercular Cortex
Social Cognition	Planum Temporale	Frontal Pole	**Temporal Occipital Fusiform Cortex**
Emotion Processing	Planum Temporale	Frontal Pole	Postcentral Gyrus

According to the results, we find there is a correlation between the predictable ROIs and the type of task. In all four tasks, we found there are some common areas that are more predictable, such as Frontal Pole, which is considered be involved with working memory [26], Planum Temporale, one of the most important functional areas for language [27], Postcentral gyrus, etc. All these common areas are involved with some behaviors taken in these kinds of task, because subjects certainly watch the monitor, use their working memory, or read some texts or pictures when being scanned by functional MRI machine. However, what is more telling is that those different predicable areas with highest scores in each task. For instance, only in language task, inferior division of Lateral Occipital Cortex are easily to be predicted, which may contributed to the large number of text volume in the task. Another evidence is that Temporal Occipital Fusiform Cortex, which plays a important role in face and body recognition [28], is highly predicable only in social cognition task, in which subjects were showed with shapes that may suggest human faces to them. To conclude, there are some different predicable areas according to various stimuli included in various task, which may infer that functions of those predicable areas are related with the given stimuli.

4.3 Contributive Areas

Another viewpoint of the results is to inspect these features we used to regress. Features are selected based on univariate linear regression tests and the weights of selected features refer to F values. The most contributive features, which are actually the subjects' brain matter volumes of ROIs, are found varied from ROI to ROI they contribute to. For example, in gambling task, we list top 3 contributive areas to the top 3 predicable areas, in figure 6.

We may say their is structurally correlation between the most contributive areas and predicable areas they contribute to. We find all contributive areas are concentrated in a relatively narrow part of brain and the predicable area they contribute is surrounded by them. However, we have no evidence to confirm if predicable areas and their contributive areas are functionally interrelated due to lack of white matter fiber tracts information, even though some of them are structurally adjacent.

The experiments results shows that our predictions with SVM were better than average predictions in some ROIs, which indicates there are correspondence between structure and activity in some certain areas.

5. Conclusion

In this paper, we discussed an approach to predict between-subject variability of brain activities and conducted the experiment on a open dataset to observe the prediction accuracy. We find that there is, assuredly, correspondence between brain structure and brain activities. The volume of some areas of subject brain interferes with the activation level of some areas during certain task. There are some limitations in this paper. Firstly, we were not able to discuss why most contributive features from input data are fixed. Besides, we didn't deal with the correlations between ROIs, anatomically or functionally, as our input data, which is also important as tissues are usually activated simultaneously. We may discuss these topics in the future.

6. Acknowledgement

This work was supported in part by the following projects: Grants-in-Aid for Scientific Research (Nos. 15H01718, and 26700009) from MEXT of Japan, and ImPACT program (Actualize Energetic Life by Creating Brain Information Industries) from CAO of Japan.

References

[1] Aaron G Filler. The history, development and impact of computed imaging in neurological diagnosis and neurosurgery: Ct, mri, and dti. *Nature Precedings*, 7(1):1–69, 2009.

[2] Donald W McRobbie, Elizabeth A Moore, Martin J Graves, and Martin R Prince. *MRI from Picture to Proton*. Cambridge university press, 2006.

[3] Scott A Huettel, Allen W Song, and Gregory McCarthy. *Functional magnetic resonance imaging*, volume 1. Sinauer Associates Sunderland, 2004.

[4] Philippe Fossati, Stephanie J Hevenor, Simon J Graham, Cheryl Grady, Michelle L Keightley, Fergus Craik, and Helen Mayberg. In search of the emotional self: an fmri study using positive and negative emotional words. *American Journal of Psychiatry*, 2014.

[5] Mariko Osaka, Naoyuki Osaka, Hirohito Kondo, Masanao Morishita, Hidenao Fukuyama, Toshihiko Aso, and Hiroshi

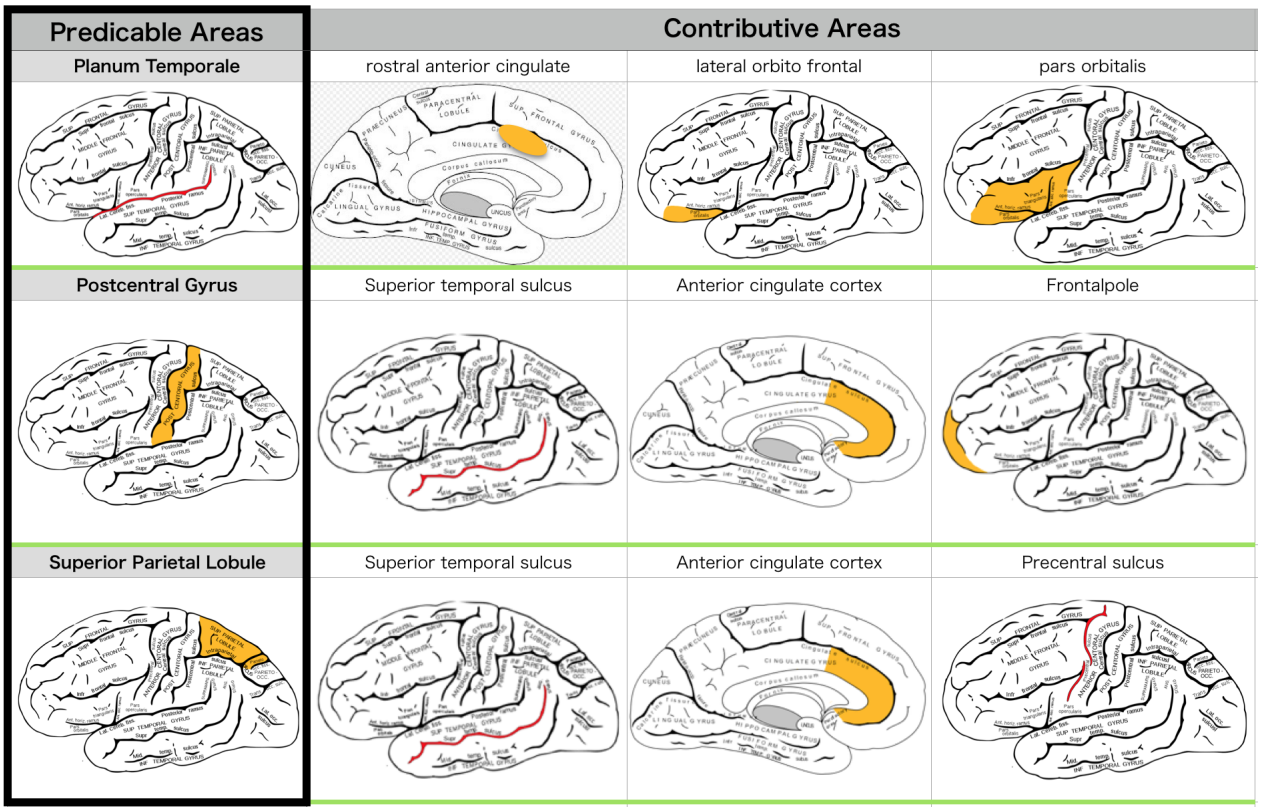

Figure 6: Predictable Areas and their top 3 contributive areas

Shibasaki. The neural basis of individual differences in working memory capacity: an fmri study. *NeuroImage*, 18(3):789–797, 2003.

[6] David C Van Essen, Stephen M Smith, Deanna M Barch, Timothy EJ Behrens, Essa Yacoub, Kamil Ugurbil, WU-Minn HCP Consortium, et al. The wu-minn human connectome project: an overview. *Neuroimage*, 80:62–79, 2013.

[7] Itzhak Aharon, Nancy Etcoff, Dan Ariely, Christopher F Chabris, Ethan O'Connor, and Hans C Breiter. Beautiful faces have variable reward value: fmri and behavioral evidence. *Neuron*, 32(3):537–551, 2001.

[8] Naomi I Eisenberger, Matthew D Lieberman, and Kipling D Williams. Does rejection hurt? an fmri study of social exclusion. *Science*, 302(5643):290–292, 2003.

[9] Joshua D Greene, R Brian Sommerville, Leigh E Nystrom, John M Darley, and Jonathan D Cohen. An fmri investigation of emotional engagement in moral judgment. *Science*, 293(5537):2105–2108, 2001.

[10] Wei Qin, Jie Tian, Lijun Bai, Xiaohong Pan, Lin Yang, Peng Chen, Jianping Dai, Lin Ai, Baixiao Zhao, Qiyong Gong, et al. Fmri connectivity analysis of acupuncture effects on an amygdala-associated brain network. *Mol Pain*, 4(55):1–17, 2008.

[11] Jonas Richiardi, Hamdi Eryilmaz, Sophie Schwartz, Patrik Vuilleumier, and Dimitri Van De Ville. Decoding brain states from fmri connectivity graphs. *Neuroimage*, 56(2):616–626, 2011.

[12] Stephen M Smith. The future of fmri connectivity. *Neuroimage*, 62(2):1257–1266, 2012.

[13] John Ashburner and Karl J Friston. Voxel-based morphometry-the methods. *Neuroimage*, 11(6):805–821, 2000.

[14] Catriona D Good, Ingrid S Johnsrude, John Ashburner, Richard NA Henson, KJ Fristen, and Richard SJ Frackowiak. A voxel-based morphometric study of ageing in 465 normal adult human brains. In *Biomedical Imaging, 2002. 5th IEEE EMBS International Summer School on*, pages 16–pp. IEEE, 2002.

[15] JC Baron, G Chetelat, B Desgranges, G Perchey, B Landeau, V De La Sayette, and F Eustache. In vivo mapping of gray matter loss with voxel-based morphometry in mild alzheimer's disease. *Neuroimage*, 14(2):298–309, 2001.

[16] Petra Schweinhardt, David A Seminowicz, Erik Jaeger, Gary H Duncan, and M Catherine Bushnell. The anatomy of the mesolimbic reward system: a link between personality and the placebo analgesic response. *The Journal of neuroscience*, 29(15):4882–4887, 2009.

[17] R Kanai, B Bahrami, R Roylance, and G Rees. Online social network size is reflected in human brain structure. *Proceedings of the Royal Society of London B: Biological Sciences*, 279(1732):1327–1334, 2012.

[18] Xiaochen Hu, Michael Erb, Hermann Ackermann, Jason A Martin, Wolfgang Grodd, and Susanne M Reiterer. Voxel-based morphometry studies of personality: issue of statistical model specification-effect of nuisance covariates. *Neuroimage*, 54(3):1994–2005, 2011.

[19] Yan Zhou, Fu-chun Lin, Ya-song Du, Zhi-min Zhao, Jian-Rong Xu, Hao Lei, et al. Gray matter abnormalities in internet addiction: a voxel-based morphometry study. *European journal of radiology*, 79(1):92–95, 2011.

[20] René Riedl, Marco Hubert, and Peter Kenning. Are there neural gender differences in online trust? an fmri study on the perceived trustworthiness of ebay offers. *Mis Quarterly*, 34(2):397–428, 2010.

[21] Ryota Kanai and Geraint Rees. The structural basis of inter-individual differences in human behaviour and cognition. *Nature Reviews Neuroscience*, 12(4):231–242, 2011.

[22] Liye Yi, Jinhui Wang, Longfei Jia, Zhilian Zhao, Jie Lu, Kuncheng Li, Jianping Jia, Yong He, Chuanlu Jiang, and Ying Han. Structural and functional changes in subcortical vascular mild cognitive impairment: a combined voxel-based morphometry and resting-state fmri study. 2012.

[23] Manuel Fernández-Delgado, Eva Cernadas, Senén Barro, and Dinani Amorim. Do we need hundreds of classifiers to solve real world classification problems? *The Journal of Machine Learning Research*, 15(1):3133–3181, 2014.

[24] Mauricio R Delgado, Leigh E Nystrom, C Fissell, DC Noll, and Julie A Fiez. Tracking the hemodynamic responses to reward and punishment in the striatum. *Journal of neurophysiology*, 84(6):3072–3077, 2000.

[25] Ahmad R Hariri, Venkata S Mattay, Alessandro Tessitore, Bhaskar Kolachana, Francesco Fera, David Goldman, Michael F Egan, and Daniel R Weinberger. Serotonin transporter genetic variation and the response of the human amygdala. *Science*, 297(5580):400–403, 2002.

[26] Sam J Gilbert, Stephanie Spengler, Jon S Simons, J Douglas Steele, Stephen M Lawrie, Christopher D Frith, and Paul W Burgess. Functional specialization within rostral prefrontal cortex (area 10): a meta-analysis. *Journal of cognitive neuroscience*, 18(6):932–948, 2006.

[27] Bruno Dubuc. The brain from top to bottom. 2002.

[28] Isabel Gauthier, Pawel Skudlarski, John C Gore, and Adam W Anderson. Expertise for cars and birds recruits brain areas involved in face recognition. *Nature neuroscience*, 3(2):191–197, 2000.